CrystEngComm

PAPER

Cite this: *CrystEngComm*, 2018, **20**, 5718

Significance of crystal habit sphericity in the determination of the impact sensitivity of bistetrazole-based energetic salts†

Sergey V. Bondarchuk

The effect of crystal growth morphology on impact sensitivity is described quantitatively. A simple theoretical background is presented to distinguish sensitive and insensitive materials with respect to their crystal habits. As a quantitative measure of impact sensitivity, crystal habit sphericity (Ψ) is introduced and the appropriate theoretical background is presented. The corresponding computational support for this approach is performed for 20 crystalline energetic salts based on 5,5′-bistetrazole derivatives, novel high-performance nitrogen-rich explosives. Along with the Ψ values, the corresponding decomposition temperatures, chemical hardness, energy content, and the average number of electrons per atom are also used in the regression equation yielding the sensitivity function Ω. A simple correlation of experimentally measured impact energies (in J) with the product ΨT_{dec}^2 provides a rather good correlation coefficient (R^2 = 0.78), while the function Ω, comprising all the above-mentioned properties has better correlation (R^2 = 0.82). The maximum absolute deviation of the predicted impact energies does not exceed ±15 J. The mean and median of the differences between the predicted and experimental values equal zero and 0.5 J, respectively.

Received 8th July 2018,
Accepted 15th August 2018

DOI: 10.1039/c8ce01117f

rsc.li/crystengcomm

Introduction

Qualitatively, the influence of crystal habits on impact sensitivity (IS) has been known for more than a half-century.[1] Thus, according to the generally accepted "hot spot" theory, the plate-like crystal habits should disfavor the risk of formation of hot spots. Moreover, the shape, size and arrangement of crystals also influence the IS.[2–5] This supposition was recently proven by measuring the IS for plate- and rod-like crystals of 3,4-bis(3-nitrofurazan-4-yl)furoxan (DNTF) grown in H_2O/AcOH and H_2O/EtOH solvents, respectively.[6] A similar effect of the crystal morphology was recently observed for co-crystals of hexahydro-1,3,5-trinitro-1,3,5-triazine (RDX) and 2,4,6,8,10,12-hexanitro-2,4,6,8,10,12-hexaazaisowurtzitane (CL-20).[7] These bar-shaped co-crystals exhibit lower IS compared to raw CL-20 particles being irregular polyhedrons.[7]

It is also known that solvents applied for re-crystallization play a crucial role in the resulting crystal habit morphology and, hence, the impact sensitivity.[8] A number of molecular dynamics simulations in terms of the modified attachment energy (AE) method are presented in the literature where the crystal growth morphologies of energetic materials are predicted in various solvents.[9–15] Often, re-crystallization leads to spheroidization of the sample in accord with the "dissolution-precipitation principle", by which the edges of a crystal are preferentially dissolved.[16] As a measure of such spheroidization, the length/diameter ratio (L/D) was used.[9,17] It was found that the sample particles with the smallest L/D ratios are the most insensitive. This result, however, may be ascribed to significant purification of the samples (≥99.90%) and removal of internal defects, namely, impurities and voids.[9] The latter can be responsible for the hot spot formation mechanism including void collapse or friction.[18] For example, the crystalline samples with smoother surfaces demonstrate reduced viscosity and, hence, a lower shock sensitivity originating from the hot spot formation due to friction at the crystal edges.[19,20]

The L/D ratio reflects the deviation of a crystal habit from an ideal sphere with respect to one selected direction; therefore, it is the most appropriate for the determination of the

Department of Chemistry and Nanomaterials Science, Bogdan Khmelnitsky Cherkasy National University, blvd. Shevchenko 81, 18031 Cherkasy, Ukraine. E-mail: bondchem@cdu.edu.ua

† Electronic supplementary information (ESI) available: Crystal packing, structural parameters, crystal orbitals and habits, habit properties, decomposition schemes and separate correlations. See DOI: 10.1039/c8ce01117f

habit ellipsoidization degree. Meanwhile, in the case of highly irregular shapes, it is scarcely applicable. Thus, another quantity was introduced to characterize the shape of the crystalline samples, namely, the crystal habit circularity C (eqn (1)).[21]

$$C = 4\pi\frac{S}{P^2}, \quad (1)$$

where S is the area of the crystal projection on a certain plane and P is the crystal projection perimeter.

Of course, the two abovementioned quantities have serious disadvantages because these do not take into account the real three-dimensional shape of the sample. For instance, the L/D ratio for a sphere (with radius r) and a cube (with side $2r$) is the same. Meanwhile, the C values for these sphere and cube structures differ and are equal to 1 and $\pi/4$, respectively. To our knowledge, there are no publications in the literature introducing a quantity, which reflects the deviation of the crystal habit from an ideal sphere in three dimensions. The only exception is our two recent papers on the theoretical study of phenyl diazonium chloride (PDC) and tetrafluoroborate (PDT) crystalline salts[22] as well as aromatic, aliphatic, and heterocyclic nitro and nitrato compounds.[23] It was found qualitatively that the crystal habit sphericity (Ψ) can serve as a measure of IS. This quantity can be expressed as eqn (2).

$$\Psi = \frac{S_{\text{cryst}}}{6^{2/3}V_{\text{cryst}}^{2/3}\pi^{1/3}}, \quad (2)$$

where S_{cryst} and V_{cryst} are the surface and volume of a crystal habit, respectively. The Ψ value determines the degree of the crystal habit deviation from a sphere of the same volume. For an ideal sphere, the Ψ value equals 1 and for crystals, which strongly expand in one or two dimensions, the value of Ψ is higher than 1.

We have found that the more sensitive PDC crystal habits have lower Ψ values than those of the insensitive PDT ones.[22] This was in complete agreement with our preliminary theoretical consideration concerning the hot spot formation mechanism. Thus, in the present paper, we have developed a theoretical background for this mechanism and supported it with calculations using 20 nitrogen-rich energetic salts with experimentally measured IS values. These salts are derivatives of 5,5′-bistetrazole containing different onium type organic and inorganic cations (Chart 1). Salt **1** is the known high-performance explosive dihydroxylammonium 5,5′-bistetrazole-1,1′-diolate (TKX-50), which is a promising green explosive, an alternative to RDX.[24]

Computational details

Due to the great variety of methods for the prediction of crystal habits, choosing the appropriate one is crucial. As it follows from the literature, different methods can provide a rather good prediction of crystal growth morphology with varying success. Among them we can highlight the purely geometry-based methods based on the Bravais–Friedel–Donnay–Harker (BFDH) model.[25–28] These methods, however, are less important since they do not take into account the energy aspects of the growth kinetics. Also, the Hartman–Perdok (HP) method, which is based on the periodic bond chain (PBC) analysis.[29] The propagation vector ($\vec{R}_{\text{p}}$) method,[30] which is based on the centre of mass of the molecular basis. In this method, the projection of the propagation vector on a crystal face determines the growth rate of the crystal plane (R_{hkl}) eqn (3).

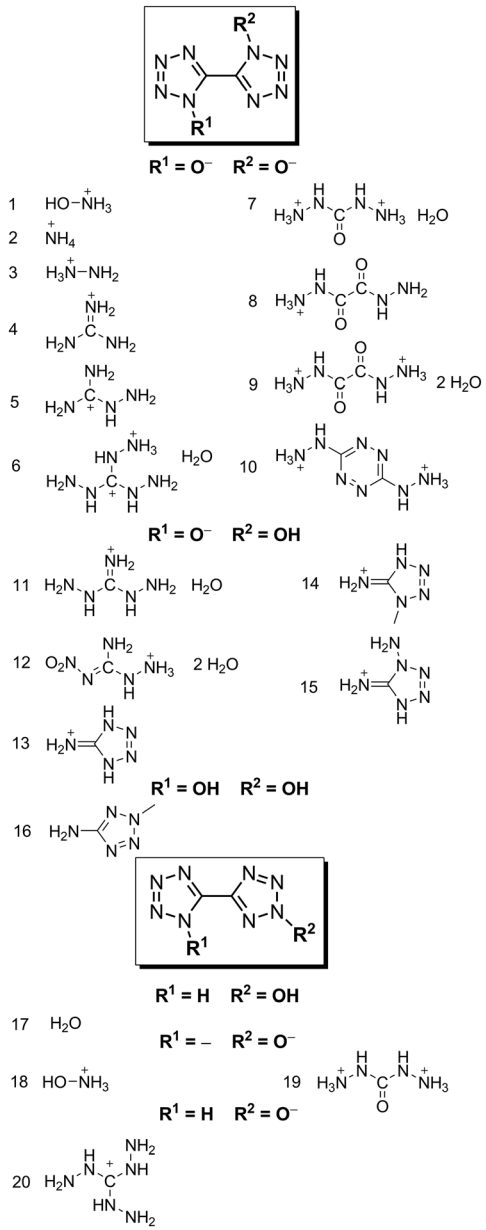

Chart 1 Chemical structures of the studied energetic salts.

$$R_{hkl} = \frac{1}{\left|\vec{R}_{\text{p}}\left(h\hat{i} + k\hat{j} + l\hat{k}\right)\right|} \quad (3)$$

Another important method is the spiral growth model originally developed by Burton–Cabrera–Frank (BCF).[31]

According to this method, the growth rate (G) of a crystal can be expressed as eqn (4).

$$G = \frac{h}{\tau}, \quad (4)$$

where h is the step height (interplanar distance of a face), and τ is the characteristic rotation time of the spiral (the time for a full turn of a spiral). The calculations using eqn (4) require a set of additional properties (edge critical length, rotation time, angle between edges, step velocity, kink and surface energy, kink density and rate) to be calculated.[32–34] An improvement of the BCF method by accounting the effect of surface relaxation on habit controlling energies and growth morphology was also proposed.[35,36] But the application of the HP method[37] for organic crystals, proposed by Hartman and Bennema,[38] which is based on the attachment energy, seems to be the most popular, especially taking into account the recent modification allowing the prediction of the growth morphology in various solvents.[9–15]

The crystal structures of the studied salts (Chart 1) were taken from ref. 24 (salt **1**), ref. 39 (salts **2–16**) and ref. 40 (salts **17–20**). We applied the AE method for these crystal structures to obtain their crystal habits. According to the AE method, the morphology of a given crystal is deduced by the center-to-plane distance assigned to the dominant crystal surface, which is proportional to relative growth rate. The attachment energy (E_{att}) is defined as the released energy by the addition of a growth slice to a growing crystal surface.[41] Thus, E_{att} is calculated as eqn (5):

$$E_{att} = E_{latt} - E_{slice}, \quad (5)$$

where E_{latt} is the lattice energy of the crystal, E_{slice} is the energy of a growth slice with thickness d_{hkl}, which must fulfill the extinction rules of the space group of the crystal.

The crystal graphs were computed using COMPASS (condensed-phase optimized molecular potentials for atomistic simulation studies) forcefield[42] with the Morphology Tools module.[43] The weakest energy at the initial step was set to be equal to −2.494 kJ mol^{-1} (thermal energy at room temperature). During the calculation of E_{att}, crystal growth was allowed along the planes with maximum Miller indices (3 3 3).

For calculating the energy content (E_c),[44] the asymmetric cells were first relaxed using the CASTEP (Cambridge Serial Total Energy Package) code[45] as implemented in the Materials Studio 7.0 suite of programs.[43] A norm-conserving pseudopotential (NCP) constructed for the pure exchange-correlation functional PBE (Perdew–Burke–Ernzerhof)[46] was applied for cell optimization. For the PBE/NCP approach, the long-range effects were taken into account using the Grimme form of the damped C_6 term.[47] Convergence tests revealed a value of 830 eV (61 Ry) as the sufficient energy cutoff for the applied plane wave basis set. Sampling of the Brillouin zone was performed using k-point grids generated using the Monkhorst–Pack scheme with the separation of k-points equal to 0.08 Å^{-1}. Optimization of nonperiodic structures (CO_2, H_2O, N_2, *etc.*) was performed using supercells which provided intermolecular spacings of not less than 25 Å.

Chemical hardness (η) values were calculated according to eqn (6):[48]

$$\eta = I - A = -E_{HOCO} + E_{LUCO}, \quad (6)$$

where I, A, E_{HOCO} and E_{LUCO} are the ionization energy, electron affinity, energy of the highest occupied (HOCO) and the lowest unoccupied (LUCO) crystal orbitals, respectively. The E_{HOCO} and E_{LUCO} values were calculated at the PBE/TNP level of theory using the DMol^3 code[49] as a part of the Materials Studio 7.0 program suite.[43]

Results and discussion

Theoretical background

Recently, we have found that a few solid-state properties of a number of aromatic, aliphatic, and heterocyclic nitro and nitrato compounds correlate well with the corresponding impact sensitivities.[23] These criteria are the following: triggering pressure (P_{trigg}), stored energy content (E_c), the average number of electrons per atom (N_F), melting points (T_m) and crystal habit sphericity (Ψ). On the basis of these five quantities, we have developed an empirical function (Ω), which correlates with impact sensitivity (eqn (7)).[23]

$$\Omega = \frac{\Psi T_m^2}{N_F^7} \exp\left(\frac{P_{trigg}}{1000}\right) \exp\left(\frac{E_c}{100}\right) \quad (7)$$

The exponents P_{trigg} and E_c are both close to 1 in eqn (7).[23] Additionally, the search for P_{trigg} values is a rather time-consuming and computationally expensive procedure which requires a few cell relaxation and band structure calculations to be performed. Also, N_F is a constant for any single molecule and can be easily calculated on a sheet of paper. In this

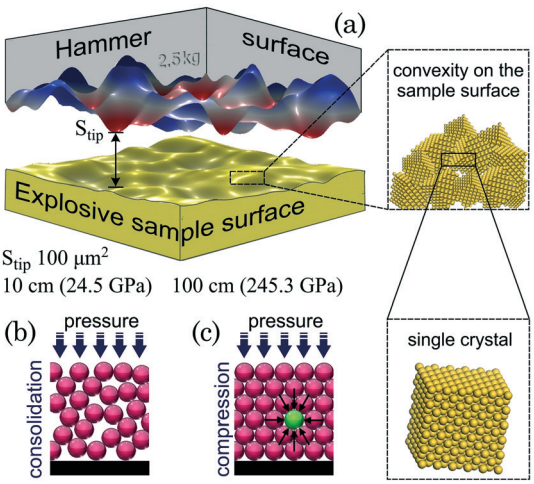

Fig. 1 Graphical representation of the processes caused by the contact of a hammer surface with an explosive sample surface.

work, only valence electrons in the utilized NCPs are taken into account. These are the following: $2s^2 2p^2$ for carbon, $1s^1$ for hydrogen, $2s^2 2p^3$ for nitrogen and $2s^2 2p^4$ for oxygen. Thus, Ψ, T_m and N_F appear to be the most important quantities in eqn (7).

The influence of crystal habit sphericity can be graphically described as in Fig. 1. It is obvious that only the restricted areas of the hammer surface first penetrate the sample, which occurs in the so-called contact zones (red areas in Fig. 1a). If one assumes that the area of a contact zone tip is 100 μm^2, then the pressure caused by the fall of a 2.5 kg hammer will be tens to hundreds of gigapascals (Fig. 1a). Such pressures are more than enough to narrow the band gap and allow the thermal electron excitation of the conduction band leading to the decomposition of molecules or ions in the crystal.[22,23,50,51]

Under impact loading, two consecutive processes take place, namely, consolidation and compression. During consolidation, no significant pressure rise is observed, since mechanical energy dissipates throughout the sample and transforms into heat due to friction at the crystal edges. At this stage a tighter sample is formed (Fig. 1b). Thereafter, the compression stage begins leading to a sharp rise in pressure and changes in the electronic band structure. Though impact sensitivity has anisotropic character,[52] in a real sample, separate crystals are distributed randomly. As a result, one can assume that crystal compression is isotropic (Fig. 1c). We speculate that the initial tightness of the crystalline sample can affect impact sensitivity due to the different consolidation/compression ratios. Obviously, crystal habit sphericity is responsible for the above-mentioned ratios. The arrangements of single crystals with different Ψ can be illustrated as those in Fig. 2a and b. This ratio will be higher in the case of Fig. 2b, meaning that local heating will prevail over the pressure rise. On the other hand, as we have recently shown, crystal compression is the predominant factor compared to heating.[22,23,53] Thus, crystals with high sphericity are expected to be more sensitive than those with low sphericity.

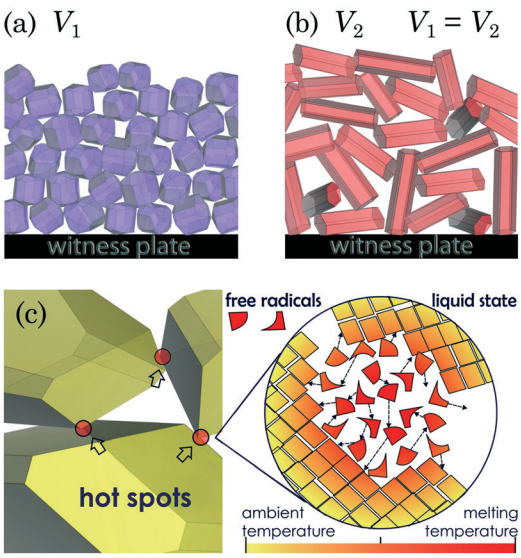

Fig. 2 Arrangement of crystals with high (a) and low (b) sphericity along with a representation of the "hot spots" (c).

Similarly, the crystal size plays an important role in impact sensitivity. Indeed, smaller crystals have a large number of contact zones between separate crystals compared to the bigger ones. Thus, the same pressure is transferred through different number of contacts and, as a result, in the case of bigger crystals, the pressure is higher. This makes bigger crystals more sensitive to impact compared to the smaller ones.

Apart from the crystal morphology, it is important to consider temperature effects. Friction at the crystal edges caused by impact loading may lead to a significant local temperature rise in the "hot spots" (Fig. 2c). When thermal electron occupation of the conduction band occurs and the excited molecules decompose to form free radicals or other reactive species, these intermediates cannot propagate a chain reaction until the crystal is melted since they are fixed at the equilibrium positions and their translational motion is restricted. Therefore, when local heating is not enough, the vibrational energy dissipates throughout the crystal and molecules return to their ground state (quenching of the hot spots). Otherwise, reactive species propagate chain decomposition of the neighboring cells resulting in an explosion (Fig. 2c). Obviously, concentration of the hot spots is the key factor affecting impact sensitivity. Thus, low-melting crystals are expected to be more sensitive than the high-melting ones.

Model calculations

In order to support these theoretical considerations, we have performed a series of first-principles calculations of 20 energetic salts, derivatives of 5,5′-bistetrazole. The chemical structures of these salts **1-20** are presented in Chart 1 and the crystal packing is illustrated in Fig. S1 in the ESI.† The optimized asymmetric cell parameters along with the experimental ones are listed in Table S1 in the ESI.† Using the NCP/PBE-Grimme/830 eV approach, we have obtained results with a rather good agreement with those from the experiment on the lattice parameters and volumes (Table S2 in the ESI†). As it follows from Table S2,† the values of δ (%) from the cell volume estimation do not exceed ±1.5% and the mean value is equal to −0.18%.

The predicted crystal habit for salt **1** (TKX-50) together with the corresponding experimental habit,[23] is illustrated in Fig. 3 and the rest of the habits for salts **2–20** are presented in Fig. S2 in the ESI.† As one can see in Fig. 3, there is a rather good reproduction of the experimental habit despite that the calculations are performed in vacuum and the experimental crystal was precipitated from an aqueous solution.[23] The only extra surface (0 2 0) appeared to be stable in vacuum compared to those in aqueous solutions; however, its relative area (S_{rel}) is only 6.42% (Table 1). The numerical data on all morphologically important surfaces of salt **1** are listed in Table 1, and the data for all the rest of the salts are listed

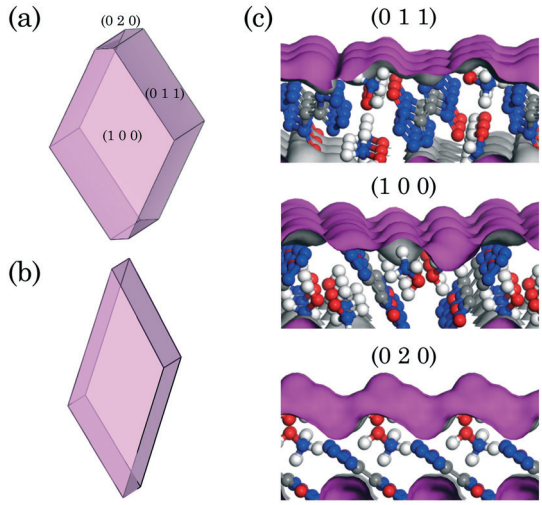

Fig. 3 The calculated (a) and experimental (b) crystal morphology of TKX-50; the corresponding Connolly surfaces (c).

Table 1 The selected crystal habit parameters for TKX-50 in vacuum predicted using the AE model

(*hkl*)	*M*	E_{att} [a]	R_{hkl}	S_{rel} (%)
(0 1 1)	4	−17.53	1.00	64.24
(1 0 0)	2	−22.51	1.28	29.34
(0 2 0)	2	−30.00	1.71	6.42

[a] In kJ mol^{-1}.

in Table S3 in the ESI.† Note that *M* is the facet multiplicity and R_{hkl} is the relative growth rate.

The reason why the calculated and experimental habits are similar is in the nature of the stable surfaces. In Fig. 3c, we have presented the calculated Connolly surfaces for salt **1**. Remarkably, these are rather smooth without large voids and convexities. In this case, the ratio of the solvent-accessible area to the corresponding surface area (the *S* parameter)[6] is close to 1. A low value of *S* means that the solvent adsorption is less favorable. As a result, the vacuum morphology can be effectively used to calculate Ψ, and there is no need to perform calculations on the crystal morphology from solutions which is a rather expensive procedure.

Thus, the calculated Ψ values for the studied energetic salts are listed in Table 2. A simple correlation of Ψ with the experimental impact energy values (Table 2) provides a poor correlation coefficient (R^2 = 0.20). A similar, but slightly better, correlation is observed for the T_{dec} values (R^2 = 0.30). But the product ΨT_{dec} correlates much better with IE and gives R^2 = 0.65. Thus, we can conclude that the crystal morphology and decomposition temperatures are important factors in the determination of impact sensitivity in the family of the bistetrazole-based energetic salts. As a result, one can improve the impact sensitivity of such salts using re-crystallization from the solvents providing larger values of Ψ.

In order to improve the correlation, we have analyzed three additional properties, namely, N_F, η and E_c, which we have recently proposed to be used in such correlations.[23,53] As we have mentioned above, N_F can be calculated manually and this quantity is inversely proportional to IE. In the case of aromatic, aliphatic, and heterocyclic nitro and nitrato compounds,[23] the correlation of the N_F values provided a better R^2 value compared to the present work, 0.39 *versus* 0.12, respectively. Probably, this is because thermal electron excitation plays a minor role in the decomposition mechanism of bistertrazole-based salts.

Table 2 Experimental values of impact sensitivity and the data used for its prediction

Salt	IE[a]	T_{dec}[b]	Ψ	N_F[c]	η[d]	E_c[e]	Ω
1	20	494	1.254	3.75	3.598	0.332	29.459
2	35	563	1.240	3.55	3.106	0.203	34.502
3	9	493	1.281	3.46	2.814	0.238	25.371
4	>40	547	1.320	3.44	3.433	0.100	39.483
5	40	501	1.534	3.39	3.299	0.140	37.535
6	15	483	1.253	3.50	3.166	0.225	26.501
7	20	493	1.134	3.66	3.321	0.214	25.096
8	20	497	1.307	3.67	2.974	0.183	26.233
9	40	495	1.604	3.65	2.903	0.171	31.337
10	40	453	1.657	3.87	1.430	0.351	12.620
11	12	477	1.211	3.53	3.292	0.217	25.728
12	10	413	1.817	3.76	2.998	0.259	24.792
13	4	497	1.207	4.09	3.202	0.349	23.440
14	6	465	1.298	3.85	3.182	0.324	23.295
15	2	443	1.191	4.00	3.195	0.360	18.737
16	8	428	1.384	3.63	3.420	0.265	23.939
17	4	445	1.225	4.00	3.670	0.288	22.321
18	20	456	1.406	3.65	3.702	0.266	29.714
19	3	487	1.169	3.68	3.702	0.198	27.946
20	3	474	1.215	3.50	3.134	0.224	24.498

[a] In J. [b] In K. [c] In e$^-$ per atom. [d] In eV. [e] In eV per atom.

Meanwhile, the E_c values are calculated according to the known H_2O–CO_2 arbitrary.[44] To construct the appropriate equation for a molecule, one must know the oxygen balance (OB, %). The OB values are listed in Table S2 in the ESI.† As one can see in Table S2,† salts **1**–**20** possess strongly negative OB values. The H_2O–CO_2 arbitrary equations for all the studied energetic salts of the general formula ($C_iH_jN_kO_l$) can be divided into three types according to the following structural criteria:

a) $l = j/2$ (salts **1**, **9**, **17**)

$$C_iH_jN_kO_{j/2} = iC + j/2H_2O + k/2N_2$$

b) $2j < l$ (salt **12**)

$$C_iH_jN_kO_l = (i - ((l - j/2)/2))C + (l - j/2)/2CO_2 + j/2H_2O + k/2N_2$$

c) $2j > l$ (the remaining salts)

$$C_iH_jN_kO_l = i - ((j - 2l)/4)C + (j - 2l)/4CH_4 + lH_2O + k/2N_2$$

The calculated values of E_c are listed in Table 2 and the balanced equations are presented in Table S4 in the ESI.† The correlation of exp(E_c) with IE is also noticeable and it provides an R^2 = 0.24.

Recently, we have developed a unified model of the impact sensitivity of metal azides, which is similar to eqn (7) but includes η as an additional atomic property.[53] This parameter comes from the known principle of maximum hardness, according to which a reactant is preferably transformed into a chemically harder product. In other words, a chemically hard crystal is harder to decompose, meaning the η values are proportional to IE. The calculated values of η are listed in Table 2. Thus, using the above-mentioned crystalline properties, we have developed an empirical model for impact sensitivity of bistetrazole-based energetic salts, which can be expressed as eqn (8).

$$\Omega = \frac{\Psi T_{dec}^2 \eta}{N_F} \exp\left(\frac{E_c}{100}\right) \quad (8)$$

The correlation of the Ω function with the experimental values of IE is illustrated in Fig. 4. Using the following regression equation: IE = 2.414Ω − 49.372, one can easily predict impact energies with an estimated standard error (SE) of 1.38. Several other statistical criteria for the correlation between the calculated and experimental values of IE are presented as the inset in Fig. 4 (SD stands for standard deviation). We should stress that the experimental value of IE for salt **4** is given ambiguously (>40 J).[39] Indeed, according to eqn (8), this value is expected to be 46 J being a good example of the reliability of the developed sensitivity model.

The correlation in Fig. 4 includes only nineteen salts since the Ω value for salt **10** is dramatically lower (12.620) compared to the rest of the values. This is related with the η value (Table 2), which strongly differs from the others (η = 1.430 eV). To find out the probable reason for such a difference, we have plotted the frontier crystal orbitals, HOCO and LUCO, for the studied salts. Remarkably, these orbitals have the same nature for all the salts except for **10**. Fig. 5 shows the orbitals for salts **10** and **1** as examples. As it follows from Fig. 5, for salt **1**, the HOCO and LUCO are the π-type orbitals localized on the dianions with negligible contribution from the cations. In the case of salt **10**, the main contribution of

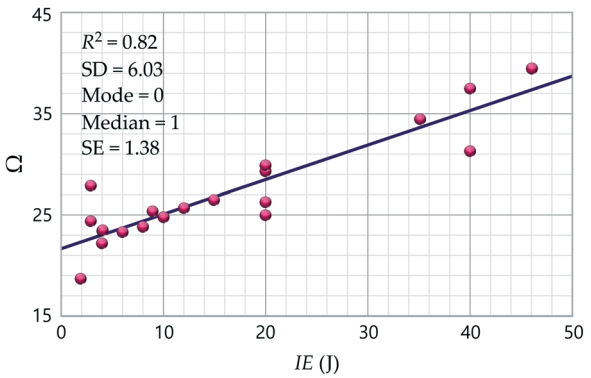

Fig. 4 The correlation of experimental impact sensitivity with the Ω function.

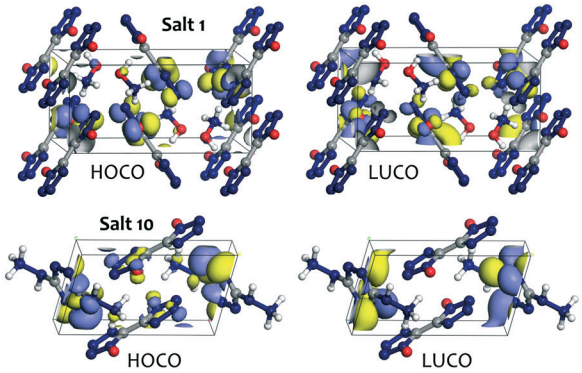

Fig. 5 The frontier crystal orbitals for salts **1** and **10**.

the HOCO and LUCO is on the dications. This can change the mechanism of pressure induced electron transition followed by decomposition of the crystal.[22,23]

Conclusions

In summary, we have presented in this paper a model of impact sensitivity for bistetrazole-based energetic salts in terms of recently proposed criteria.[22,23,53] The model revealed that the crystal habit sphericity, along with the melting temperature, is the main determinant of impact sensitivity. Remarkably, simply accounting the product ΨT_{dec}^2 as the only criterion provides rather good correlation with IE (R^2 = 0.78). This means that the impact sensitivity of bistetrazole-based energetic salts is strongly dependent on the crystallization conditions. Varying the solvent, one can dramatically change the sensitivity of the re-crystallized salt. At the same time, separate correlations of Ψ and T_{dec} give poor values of R^2 (Fig. S3 in the ESI†) suggesting the complementary character of these solid-state properties.

In this paper, we have provided a theoretical background for this criterion in terms of the hot spot formation mechanism. According to the latter, propagation of the decomposition reaction should take place in the liquid state in the vicinity of a hot spot. Thus, accounting the melting (or decomposition) temperature is essential for impact sensitivity prediction. The developed model is an additional illustration of the conception of thermal electron excitations induced by impact loading. It seems to be scarcely possible to provide an analytical expression of impact sensitivity due to the stochastic nature of an impact event. On the other hand, the obtained correlation coefficient (R^2 = 0.82) provides a solid support for the proposed theoretical considerations. Thus, the presented model of impact sensitivity is now applied for aromatic, aliphatic, and heterocyclic nitro and nitrato compounds,[23] metal azides[53] and bistetrazole-based energetic salts.

Applicability of the developed model to the friction sensitivity phenomenon is less probable. Correlation of the Ω values with the friction sensitivities is noticeable, but the value of R^2 is too low (Fig. S3 in the ESI†). Probably, this can

be caused by a lack of description of the crystal surface. Thus, a more detailed study is required to develop an appropriate empirical model.

Conflicts of interest

There are no conflicts to declare.

Acknowledgements

This work was supported by the Ministry of Education and Science of Ukraine, Research Fund (Grant No. 0117U003908).

Notes and references

1 F. P. Bowden and A. D. Yoffe, *Initiation and growth of explosions in liquids and solids*, Cambridge University Press, Cambridge, 1952.
2 V. W. Manner, B. C. Tappan, B. L. Scott, D. N. Preston and G. W. Brown, *Cryst. Growth Des.*, 2014, **14**, 6154–6160.
3 C. Zhang, Q. Peng, L. Wang and X. Wang, *Propellants, Explos., Pyrotech.*, 2010, **35**, 561–566.
4 H. Czerski and W. G. Proud, *J. Appl. Phys.*, 2007, **102**, 113515.
5 X. Song, F. Li, Y. Wang, C. An, J. Wang and J. Zhang, *J. Energ. Mater.*, 2012, **30**, 1–29.
6 N. Liu, Y.-N. Li, S. Zeman, Y.-J. Shu, B.-Z. Wang, Y.-S. Zhou, Q.-L. Zhao and W.-L. Wang, *CrystEngComm*, 2016, **18**, 2843–2851.
7 H. Gao, W. Jiang, J. Liu, G. Hao, L. Xiao, X. Ke and T. Chen, *J. Energ. Mater.*, 2017, **35**, 490–498.
8 A. E. D. M. van der Heijden and R. H. B. Bouma, *Cryst. Growth Des.*, 2004, **4**, 999–1007.
9 Y. Wang, X. Li, S. Chen, X. Ma, Z. Yu, S. Jin, L. Li and Y. Chen, *Materials*, 2017, **10**, 974.
10 F. Shen, P. Lv, C. Sun, R. Zhang and S. Pang, *Molecules*, 2014, **19**, 18574–18589.
11 W. Shi, Y. Chu, M. Xia, W. Lei and F. Wang, *J. Mol. Graphics Modell.*, 2016, **64**, 94–100.
12 J. Tao and X. Wang, *J. Chem. Sci.*, 2017, **129**, 495–503.
13 G. Chen, M. Xia, W. Lei, F. Wang and X. Gong, *J. Phys. Chem. A*, 2014, **118**, 11471–11478.
14 Y. Liu, W. Lai, T. Yu, Y. Ma, Y. Kang and Z. Ge, *RSC Adv.*, 2017, **7**, 1305–1312.
15 C. Schmidt and J. Ulrich, *Chem. Eng. Technol.*, 2012, **35**, 1009–1012.
16 A. M. Nguyen, A. Nordborg, A. Shchukarev and K. Irgum, *J. Sep. Sci.*, 2009, **32**, 2619–2628.
17 H. Chen, L. Li, S. Jin, S. Chen and Q. Jiao, *Propellants, Explos., Pyrotech.*, 2012, **37**, 77–82.
18 H. Czerski, M. W. Greenaway, W. G. Proud and J. E. Field, *AIP Conf. Proc.*, 2006, **845**, 1053–1056.
19 R. J. Hudson, M. Moniruzzaman and P. P. Gill, *Propellants, Explos., Pyrotech.*, 2015, **40**, 233–237.
20 H. Czerski and W. G. Proud, *J. Chem. Phys.*, 2013, **139**, 164704.
21 J. K. Miller, J. O. Mares, I. E. Gunduz, S. F. Son and J. F. Rhoads, *J. Appl. Phys.*, 2016, **119**, 024903.
22 S. V. Bondarchuk, *Int. J. Quantum Chem.*, 2017, **117**, e25430.
23 S. V. Bondarchuk, *J. Phys. Chem. A*, 2018, **122**, 5455–5463.
24 N. Fischer, D. Fischer, T. M. Klapötke, D. G. Piercey and J. Stierstorfer, *J. Mater. Chem.*, 2012, **22**, 20418–20422.
25 Z. Wang, P. Jiang and L. Dang, The morphology prediction of lysozyme crystals deduced from the BFDH law and attachment energy model based on the intermolecular interaction, *4th International Conference on Bioinformatics and Biomedical Engineering, Chengdu*, 18-20 June 2010, IEEE, vol. 2010.
26 D. S. Coombes, C. R. A. Catlow, J. D. Gale, M. J. Hardy and M. R. Saunders, *J. Pharm. Sci.*, 2002, **91**, 1652–1658.
27 S. Mirza, I. Miroshnyk, J. Heinämäki, O. Antikainen, J. Rantanen, P. Vuorela, H. Vuorela and J. Yliruusi, *AAPS PharmSciTech*, 2009, **10**, 113–119.
28 P. Bennema, H. Meekes, S. X. M. Boerrigter, H. M. Cuppen, M. A. Deij, J. van Eupen, P. Verwer and E. Vlieg, *Cryst. Growth Des.*, 2004, **4**, 905–913.
29 F. R. Massaro, M. Rubbo and D. Aquilano, *Cryst. Growth Des.*, 2010, **10**, 2870–2878.
30 H. Yadav, N. Sinha and B. Kumar, *Cryst. Growth Des.*, 2016, **16**, 4559–4566.
31 W. K. Burton, N. Cabrera and F. C. Frank, *Philos. Trans. R. Soc., A*, 1951, **243**, 299–358.
32 B. Seo, T. Kim, S. Kim, J. H. Ryu, J. Ryu, J. Yoon, W. B. Lee and Y.-W. Lee, *Cryst. Growth Des.*, 2017, **17**, 1088–1095.
33 H.-M. Shim and K.-K. Koo, *Cryst. Growth Des.*, 2014, **14**, 1802–1810.
34 Z. B. Kuvadia and M. F. Doherty, *Cryst. Growth Des.*, 2011, **11**, 2780–2802.
35 M. K. Singh and A. Banerjee, *Cryst. Res. Technol.*, 2011, **46**, 1035–1043.
36 M. K. Singh, *ChemXpress*, 2014, **3**, 74–83.
37 P. Hartman and W. G. Perdok, *Acta Crystallogr.*, 1955, **8**, 49–52.
38 P. Hartman and P. Bennema, *J. Cryst. Growth*, 1980, **49**, 145–156.
39 N. Fischer, T. M. Klapötke, M. Reymann and J. Stierstorfer, *Eur. J. Inorg. Chem.*, 2013, **2013**, 2167–2180.
40 T. M. Klapötke, M. Q. Kurz, R. Scharf, P. C. Schmid, J. Stierstorfer and M. Sućeska, *ChemPlusChem*, 2015, **80**, 97–106.
41 R. Docherty, G. Clydesdale, K. J. Roberts and P. Bennema, *J. Phys. D: Appl. Phys.*, 1991, **24**, 89–99.
42 H. Sun, *J. Phys. Chem. B*, 1998, **102**, 7338–7364.
43 *Materials Studio 7.0*, Accelrys Inc., San Diego, CA, 2013.
44 D. Mathieu, *Ind. Eng. Chem. Res.*, 2017, **56**, 8191–8201.
45 S. J. Clark, M. D. Segall, C. J. Pickard, P. J. Hasnip, M. J. Probert, K. Refson and M. C. Payne, *Z. Kristallogr. – Cryst. Mater.*, 2005, **220**, 567–570.
46 J. P. Perdew, K. Burke and M. Ernzerhof, *Phys. Rev. Lett.*, 1996, **77**, 3865–3868.
47 S. Grimme, *J. Comput. Chem.*, 2006, **27**, 1787–1799.

48 P. K. Chattaraj, U. Sarkar and D. Ranjan Roy, *Chem. Rev.*, 2006, **106**, 2065–2091.
49 B. Delley, *J. Chem. Phys.*, 2000, **113**, 7756–7764.
50 S. V. Bondarchuk and B. F. Minaev, *RSC Adv.*, 2015, **5**, 11558–11569.
51 S. V. Bondarchuk and B. F. Minaev, *Chem. Phys. Lett.*, 2014, **607**, 75–80.
52 Q. An, T. Cheng, W. A. Goddard III and S. V. Zybin, *J. Phys. Chem. C*, 2015, **119**, 2196–2207.
53 S. V. Bondarchuk, *Mater. Sci. Eng., B*, submitted.